

An Algorithm for Correcting CTE Loss in Spectrophotometry of Point Sources with the STIS CCD

Ralph Bohlin and Paul Goudfrooij
August 8, 2003

ABSTRACT

The correction for the change in sensitivity with time for the STIS CCD modes is complicated by the gradual loss of charge transfer efficiency (CTE) of the CCD. The amount of this CTE loss depends on time in orbit, the location on the CCD chip with respect to the readout amplifier, the stellar signal strength, and the background level. Primary constraints on our correction algorithm are provided by measurements of the CTE loss rates for simulated spectra (tungsten lamp images taken through slits oriented along the dispersion axis) combined with estimates of CTE losses for actual stellar spectra in the first order CCD modes. The main complication is the quantification of the roll-off of the CTE losses for weak stellar signals on non-zero backgrounds. This roll-off term is determined by relatively short exposures of primary standard stars along with the G750L series of properly exposed AGK+81D266 monitoring data, where the observed changes in response over time are primarily CTE losses and not sensitivity degradations. After accounting for CTE losses and after an iterative determination of the optical system throughput losses, the CTE correction algorithm is verified by comparing G230L MAMA fluxes of faint standard stars with G430L fluxes in the overlap region around 3000Å. For spectra at the standard reference position at the CCD center, CTE losses as big as 20% are corrected to within 1% at high signal levels and with a precision of ~2% at ~100 electrons after application of the algorithm presented here.

1. INTRODUCTION

Kimble, Goudfrooij, & Gilliland (2001, hereafter KGG) presented evidence that imperfect Charge Transfer Efficiency (CTE) of the STIS CCD causes a significant reduction in response for point-source spectroscopy. These losses are caused by radiation damage and are getting worse with time on-orbit. In order to produce correctly flux-calibrated spectra, an algorithm is required to correct for charge transfer inefficiency ($CTI = 1 - CTE$).

2. THE DIRECT MEASUREMENTS OF CTI

Figure 6a of KGG shows the CTI vs. total “gross” charge, G , in a standard 7-pixel spectroscopic extraction height for a sparse field at 2.6 years after launch. In the mean time, T. Brown (2003, private communication) performed measurements of similar data for 3.12 and 3.66 years in orbit with $B = 0.25$ electrons per pixel. The fit of our algorithm (described below) to the average of those two (3.12 and 3.66 year) data points appears in Figure 1 for an observation at the standard central reference position. This fit is relevant to a time of 3.4 years post-launch, i.e., at year 2000.6 and is applicable to each individual readout of a spectroscopic observation with the CCD.

The measured gross signal, G , determines the true gross signal, G_T , in electrons in the 7-pixel extraction height as mentioned below in Eq. (1). The dark current, as well as the spurious charge (0.5 electrons at gain=1 and 5.0 electrons at gain=4; see Goudfrooij & Walsh 1997), contribute to the filling of charge traps on the CCD and, hence, should be included in the measured gross signal G :

$$G_T = G / (1 - CTI)^{YBIN * ((1024/YBIN) - Y)}, \quad (1)$$

where the row number Y starts with 1 at the bottom of the chip, and $YBIN$ is the on-chip binning factor along the Y direction. Figure 1 is for $Y = 512$ and $YBIN = 1$.

Because the CTI increases linearly with time, the $CTI(G, t)$ at time t in decimal years is

$$CTI(G, t) = 0.0355 G^{-0.750} \{(t - 2000.6)0.243 + 1\}, \quad (2)$$

where the term $0.0355 G^{-0.750}$ is the predicted CTI for zero sky, zero spurious charge, and zero dark current at 2000.6. The 0.243 constant in Eq. (2) was derived from the combination of the pre-launch sparse-field measurements of Malumuth (1996) and the similar in-flight measurements by T. Brown (2003, private communication), covering the time interval 1997.16 – 2002.79 (in years). At time 2000.6, the CTI adopted for the $B = 0.25$ signal is shown by the dashed line in Figure 1.

3. EMPIRICAL ADJUSTMENTS TO THE SIMPLE CTI CORRECTION

The dashed line in Figure 1 is an overestimate of the CTI, because even a sky as low as ~ 1 electron/pix is effective in clearing the traps for weak signals at the CCD center, which is 511 parallel transfers from the default readout amplifier (D). Therefore, a roll-off must be applied to Eq. (2) that is most effective at low signals. The reduction in CTI for $B > 0.25$ electrons per pixel must depend somehow on the ratio B/G , because Figure 2 shows less CTI for the larger signals at short wavelengths for a data set with a background level that is constant with wavelength. The rapid onset of reduced CTI with lower signal suggests a drop as $\exp(-a(B/G)^p)$, while the appropriate roll-off constants $a = 2.97$ and $p = 0.21$ in Eq. (3) are a best compromise for the weak signals of ~ 80 electrons near 1750 \AA for LDS749B (using the G230LB grating) and of 150-200 electrons in a weak 70 s exposure of G191B2B around $10,000 \text{ \AA}$ (G750L grating). The residuals for G191B2B are reduced for higher values of p , while the LDS749B residuals shown in Figure 3 increase for higher values of p . The G191B2B residuals with the adopted constants for the 70 s exposure O6IG100D0 obtained on 2002 Apr 22 are typical of longer exposures of 1020 s obtained in 1997 when the CTE losses were minimal. The complete formula for the CTI correction algorithm as a function of background B and total electrons in a 7-pix high extraction is

$$\begin{aligned} CTI(B, G, t) &= CTI(G, t) \exp\left(-2.97(B'/G)^{0.21}\right) \\ &= 0.0355 G^{-0.750} (0.243(t - 2000.6) + 1) \exp\left(-2.97(B'/G)^{0.21}\right) \end{aligned} \quad (3)$$

where B' is the sum of the sky B , the dark current, and the spurious charge (which are all included in G as well). The values for B and G are readily obtained from the output of the **x1d** routine to extract 1-D spectra (McGrath, Busko & Hodge 1999). Note that the background spectrum in **x1d** is smoothed in the spatial direction prior to subtraction; this smoothed version is the B used in Eq (3). Figure 1 shows CTI curves for backgrounds of $B = 0.5$ and 2 electrons that bracket the typical range of backgrounds in spectral images.

While Figure 2 illustrates the effect of CTI on the long-wavelength AGK+81D266 response as a function of time, Figure 4 demonstrates the efficacy of the correction per Equation 3 in removing this instrumental signature. The systematic residuals are always less than one percent, except for the very longest 2% of the wavelength coverage beyond $10,100 \text{ \AA}$. An additional correction term might be required to account for the excess scattering in the CCD substrate (the ‘‘halo’’) at wavelengths greater than $\sim 10,000 \text{ \AA}$. More calibration data is required to test the accuracy of the roll-off correction for $G < 60$ electrons. Such calibration data will be obtained during Cycle 12.

Figure 5 illustrates two cases with dramatic improvement in the overlap of MAMA/G230L and CCD/G430L fluxes after correcting both datasets for time-dependent sensitivity losses (Bohlin 1999; Stys & Walborn 2001) and the CCD data for CTE losses. The success of the correction algorithm for the stellar spectra in the globular cluster NGC 6681 is an unexpected bonus, because those data are actually taken in a crowded field with spectra of numerous stars appearing along the 52×2 arcsec slit. The mean background between the spectrum and the readout amp D is $B = 11.6$ electrons, for which application of Eq. (3) provides a good match of the CCD/G430L with the MAMA/G230L fluxes in the overlap

region. In other words, the algorithm can work for a crowded field as well as for a sparse field.

4. ACKNOWLEDGMENTS

We thank Tom Brown and Randy Kimble for providing us with their CTI measurements from the internal sparse field CTE calibration program.

5. REFERENCES

- Bohlin, R. C., 1999, STIS Instrument Science Report 99-07
- Goudfrooij, P., Walsh, J. R., 1997, STIS Instrument Science Report 97-09
- Kimble, R., Goudfrooij, P., & Gilliland, R. 2001, Proc. SPIE, 4013, p. 532 (KGG)
- Malumuth, E., 1996, STIS Pre-Launch Analysis Report #055 (available through GSFC web site at http://hires.gsfc.nasa.gov/stis/reports/reports_table.html)
- McGrath, M. A., Busko, I., Hodge, P., 1999, STIS Instrument Science Report 99-03
- Stys, D. J., Walborn, N. R., 2001, STIS Instrument Science Report 2001-01

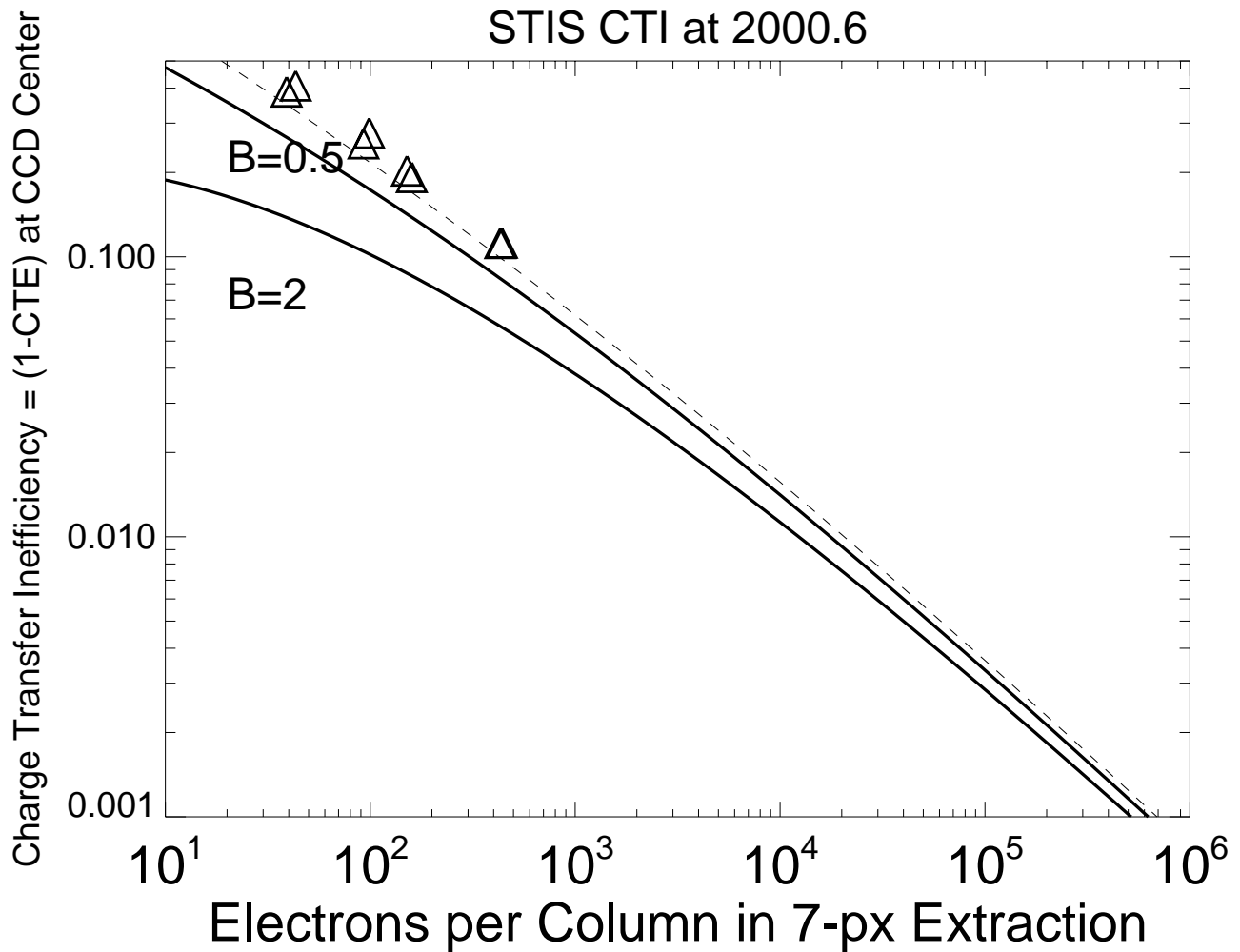


Figure 1: CTI($G, 2000.6$) at 2000.6, ie 3.4 years after launch at the CCD central default aperture position. The abscissa is G , the total gross signal (in electrons) recorded in the 7-pixel high extraction box. The dashed line is a fit to the CTI derived for artificial spectra from the internal sparse field test (triangles) that have low $B = 0.25$ electrons/pix of sky at 3.12 and 3.66 years after launch and is relevant to an image from a single readout of the CCD. The measurements (triangles) have been divided by small amounts, 0.94 and 1.07 at 3.12 and 3.66 years, respectively, to correct the data points to the mean time of 2000.6, so that the scatter within the pairs of points at each of the four electron levels is indicative of the intrinsic uncertainty. Heavy solid lines represent the CTI for background levels of 0.5 and 2 electron/pixel, which are typical for stellar spectra.

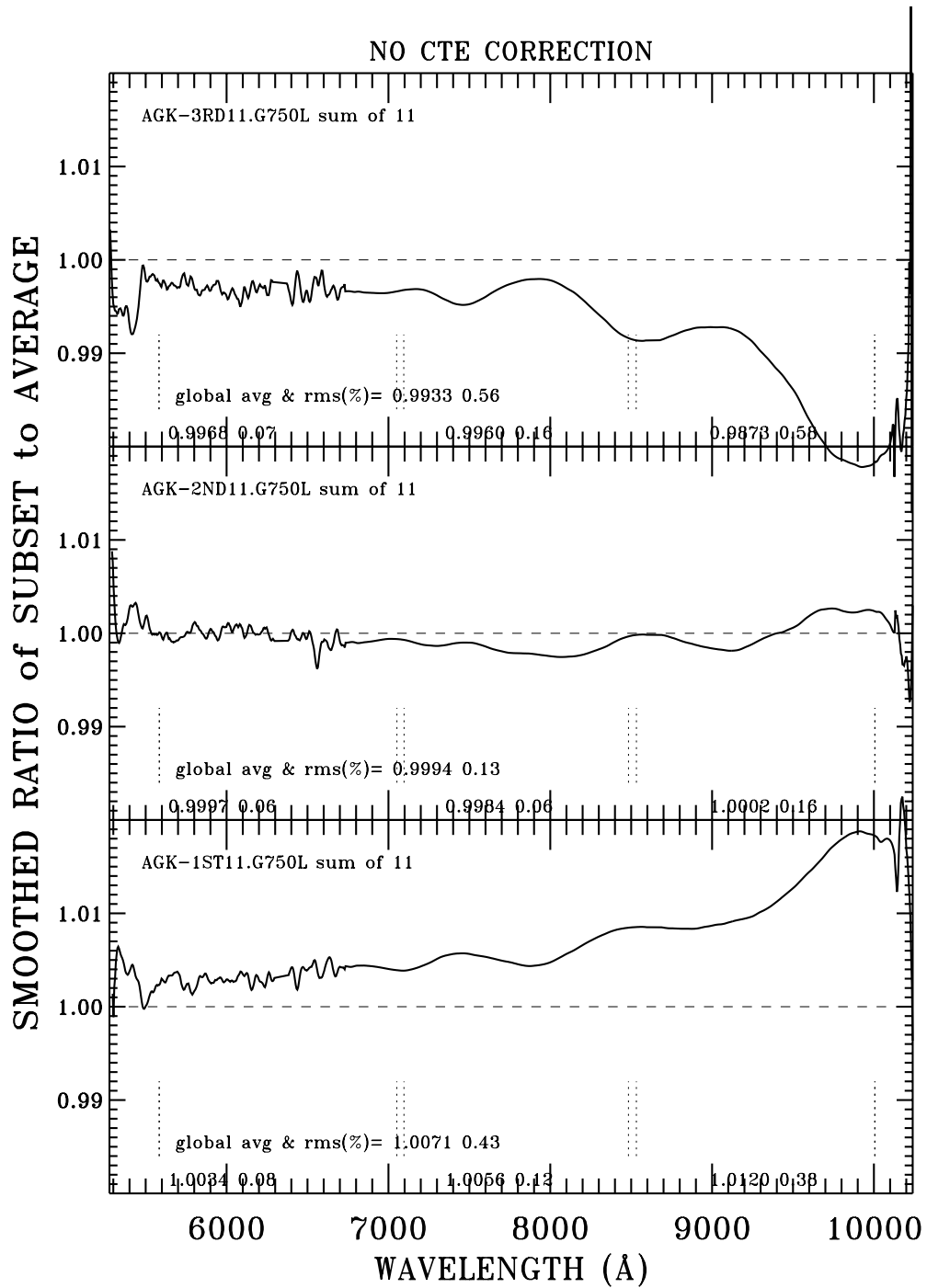


Figure 2: Average observations of the sensitivity monitor standard AGK+81D266 divided into thirds by time, where the most recent third in the top panel begins after the switch to side 2 in 2001 July. No change in sensitivity with time has been measured for G750L, and no correction for CTI has been applied. Errors bigger than +/- 1% appear at wavelengths longer than ~9400Å. The denominator is the average of all 33 G750L observations of AGK+81D266, so that the mean of all three ratios is unity at all wavelengths.

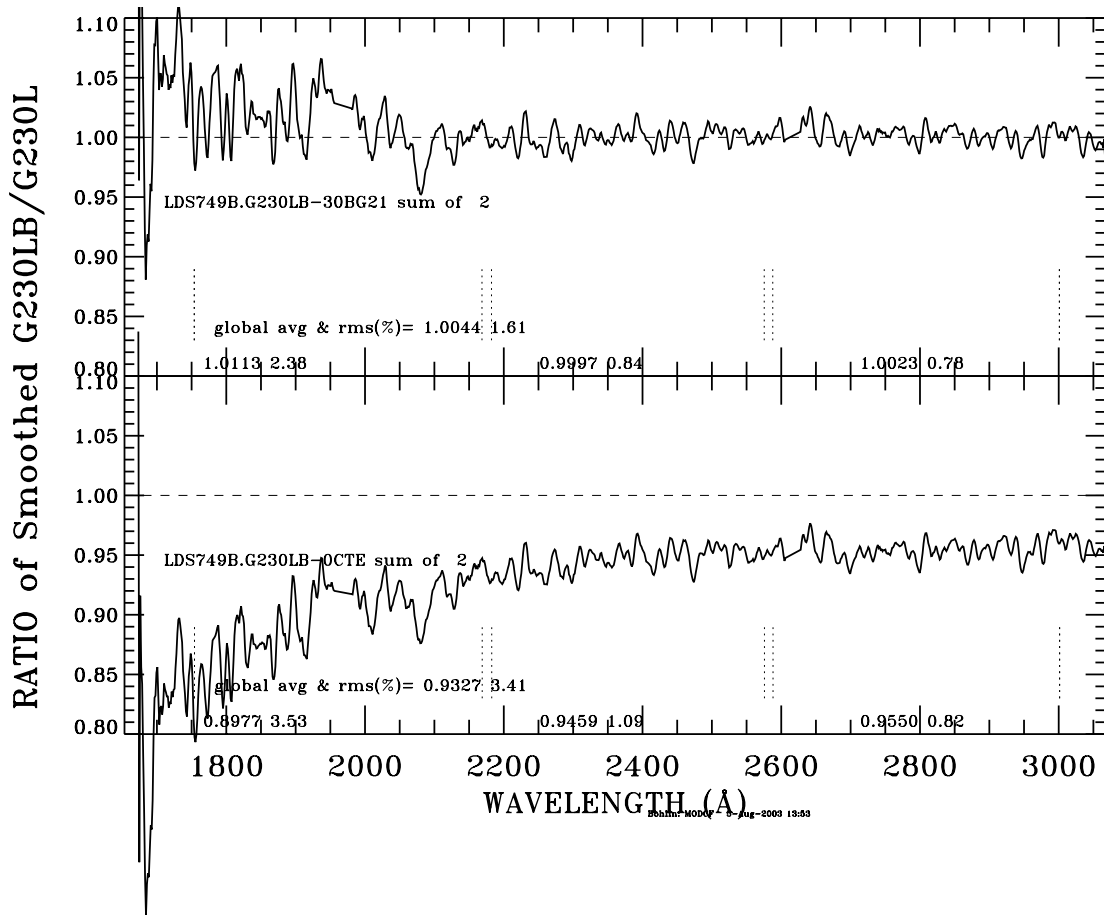


Figure 3: Ratio of the CCD/G230LB flux to the MAMA/G230L flux for LDS749B, where the G230LB CCD signal is as weak as ~ 100 electrons. Both denominator and numerator have been corrected for similar changes of sensitivity with time. The G230L observations are also adjusted for the small non-linearity in the MAMA global pulse counting rates for bright sources. The bottom panel shows the G230LB error with no CTI correction; the top panel shows the residuals for the adopted CTI algorithm. The global value and rms of the residuals are written on each panel, along with three mean and rms values for the three separate regions delineated by the vertical dashed lines. The bottom panel shows that the error of 10% (0.9002) for zero CTI correction is corrected to $\sim 1\%$ (1.00113) in the worst third of the data in the shortest wavelength bin.

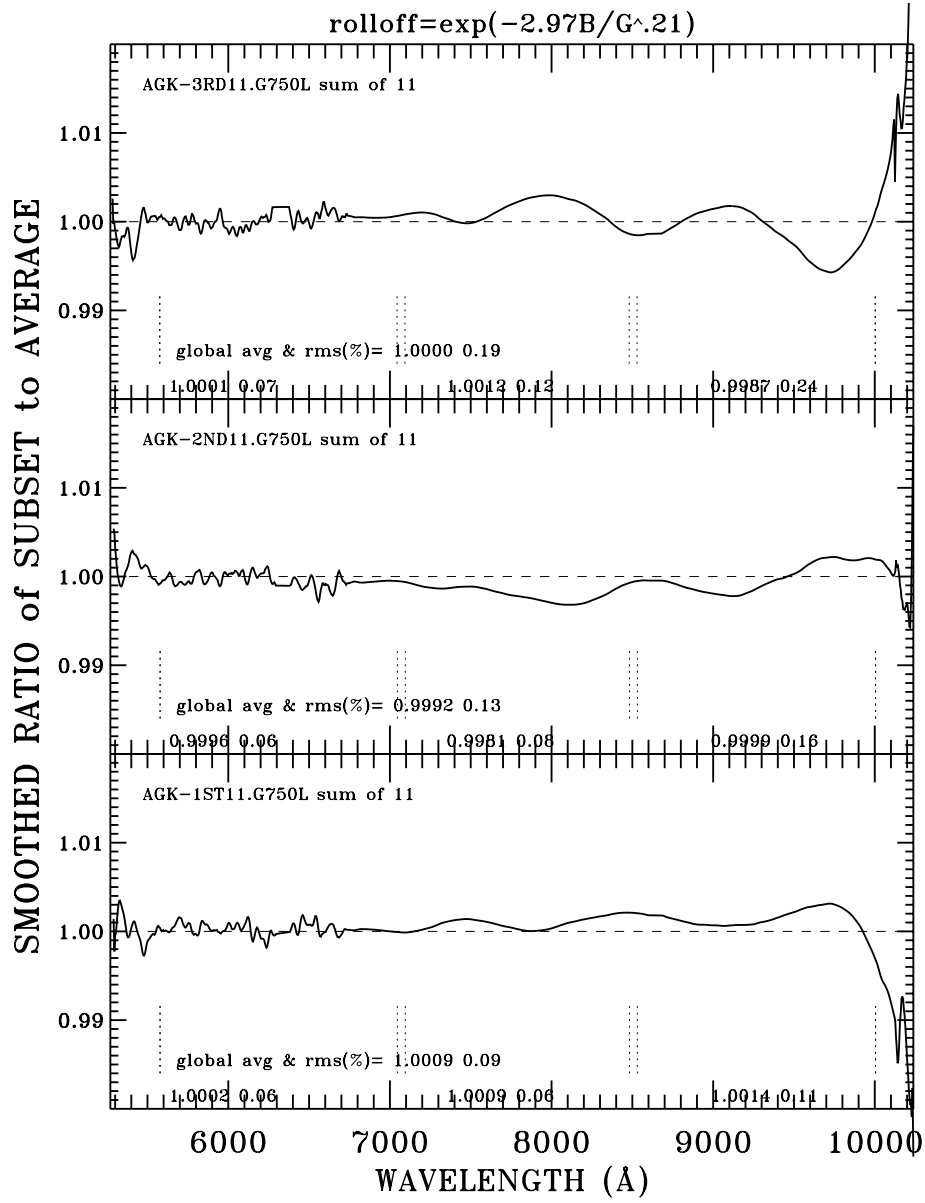


Figure 4: As in Figure 2, but AFTER application of the CTI correction specified by Eq. (3). Residuals exceed 1% only for the last 100 Å of wavelength coverage beyond 10,100 Å.

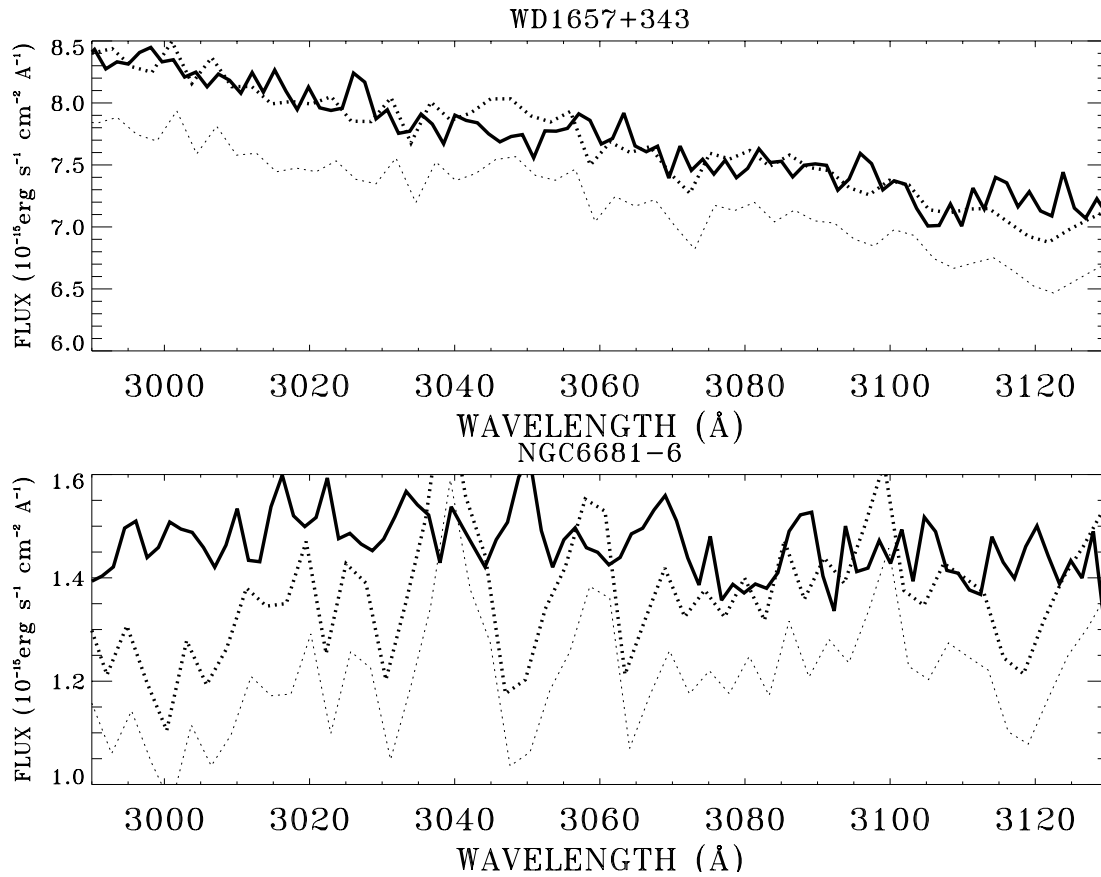


Figure 5: Flux in the overlap region of MAMA/G230L and CCD/G430L for spectra of faint standard stars that are located near the central row of the CCD. Heavy solid lines: G230L flux. Dotted lines: G430L fluxes with no correction for CTI (light dotted line) and after applying the correction algorithm from Eq. (3) (heavy dotted line). The lower panel for star 6 in the crowded field of the globular cluster NGC 6681 is typical of the results for all stars in the 52x2 arcsec slit from NGC6681-1 at row 349 to NGC6681-12 at row 707.